

Cuban coral traces annual hydrologically driven variability in $\delta^{234}\text{U}$ values since the end of the Little Ice Age

Sahra Greve¹, Norbert Frank¹, Paolo Montagna², Carlos Manuel Alonso-Hernández³, Miguel Gomez-Batista⁴, Eric Douville⁵, Sophie Warken^{1,6}

¹Institute of Environmental Physics, University of Heidelberg, Im Neuenheimer Feld 229, 69120 Heidelberg, Germany

²Institute of Polar Sciences (ISP), National Research Council, Via Piero Gobetti 101, 40129 Bologna, Italy

³IAEA Environment Laboratories 4, Quai Antoine 1er, 98000 Monaco, Principality of Monaco

⁴Centro de Estudios Ambientales de Cienfuegos (CEAC), Cienfuegos, Cuba

10 ⁵Laboratoire des Sciences du Climat et l'Environnement, LSCE/IPSL, CEA-CNRS-UVSQ, Université Paris-Saclay, F-911-91 Gif-sur-Yvette, France

⁶Institute of Earth Sciences, University of Heidelberg, Im Neuenheimer Feld 234, 69120 Heidelberg, Germany

Correspondence to: Sahra Greve (sgreve@iup.uni-heidelberg.de)

15 **Abstract.** The natural uranium isotope ratio of $^{234}\text{U}/^{238}\text{U}$ in seawater behaves conservatively at basin scale, yet it can be regionally affected by continental freshwater discharge at decadal to centennial timescales. Here, we analyse annual variations in the $^{234}\text{U}/^{238}\text{U}$ isotope ratio, expressed as ‰-deviation from radioactive equilibrium as $\delta^{234}\text{U}$, of a coral from Cuba. Over the past 237 years, the mean $\delta^{234}\text{U}$ value of the coral was 145.76 ± 0.1 ‰ ($1 \sigma_M$), which is identical to that of modern open ocean seawater, whereas the average variation over the past century has been ± 3.7 ‰. This moderate variability is, however, 20 significantly greater than the external precision and reproducibility of measurements of ± 0.55 ‰ ($2 \sigma_M$). Moreover, the $\delta^{234}\text{U}$ values coincide inversely with regional precipitation, suggesting excess ^{234}U contribution from regional freshwater runoff. The most important finding is a strong increase in annual $\delta^{234}\text{U}$ variability to ± 8.1 ‰ during the end of the Little Ice Age (LIA, 1778–1847). We suggest that the increased $\delta^{234}\text{U}$ dynamics reflect substantial excess ^{234}U contributions from the Mississippi, far greater variability in the local freshwater fluxes to the Gulf of Mexico, and/or reduced advective currents during the LIA. 25 This study demonstrates that yet unexplored variability in coral $\delta^{234}\text{U}$ records within the presently known range of seawater $\delta^{234}\text{U}$ may be attributed to local and advected freshwater sources, which opens a new pathway for reconstructing these processes over time. Moreover, it places strong constraints on the initial $\delta^{234}\text{U}$ variability of fossil corals in light of ultra-high-precision $^{230}\text{Th}/\text{U}$ dating.

1 Introduction

30 In the modern ocean, uranium is conservative, with a residence time of 200–400 ka (Ku et al., 1977; Dunk et al., 2002), far larger than the global ocean mixing timescale of approximately 1 ka, which allows for homogenization of the U content with

a conservative behaviour vs. salinity (Not et al., 2012) and isotopic composition of the world oceans. Consequently, owing to the continuous production of ^{234}U via ^{234}Th and ^{234}Pa from the decay of ^{238}U , with a half-life of 4.4683×10^9 years (Jaffey et al., 1971; Ivanovich & Harmon, 1992; Cheng et al., 2013), the activity ratio of $^{234}\text{U}/^{238}\text{U}$ (also expressed as ‰-deviation from radioactive equilibrium $\delta^{234}\text{U}$) in seawater also remains predominantly conservative (Henderson, 2002; Robinson et al., 2004a; Andersen et al., 2010).

However, seawater $\delta^{234}\text{U}$ ($\delta^{234}\text{U}_{\text{sw}}$) is in radioactive disequilibrium in the global ocean (Ku et al., 1977; Chen et al., 1986; Delanghe et al., 2002; Robinson et al., 2004a; Andersen et al., 2010; Andersen et al., 2015; Kipp et al., 2022) due to the continuous input of excess ^{234}U from rivers and submarine groundwater (Robinson et al., 2004a; Andersen et al., 2010; Li et al., 2023). Typically, these waters are enriched in ^{234}U due to the α -recoil process of radioactive decay from ^{238}U to ^{234}U , leading to preferential release of ^{234}U into the hydrological environment (Kigoshi, 1971; Chabaux et al., 2008). ^{234}U enrichment is highly variable (Dunk et al., 2002) and is influenced by physical and chemical weathering, resulting in the global ocean exhibiting an excess of approximately 15 ‰ from secular equilibrium (Ku et al., 1977; Chen et al., 1986; Delanghe et al., 2002; Robinson et al., 2004a; Andersen et al., 2010; Andersen et al., 2015; Kipp et al., 2022). A recent reassessment of the open ocean confirmed a constant $\delta^{234}\text{U}$ value of 145.55 ‰ (standard error of the mean (σ_{M}) = ± 0.28 ‰), with a range of 1.30 ‰ (Kipp et al., 2022). Modern corals have been analysed for their $\delta^{234}\text{U}$ values to confirm the $\delta^{234}\text{U}_{\text{sw}}$ uniformity observed in modern ocean far from continental sources of marine uranium (Chen et al., 1986; Delanghe et al., 2002; Robinson et al., 2004b; Andersen et al., 2010; Andersen et al., 2015; Kipp et al., 2022). Variations in the $\delta^{234}\text{U}$ values of fossil corals have been attributed to either diagenetic overprint or large-scale ice volume (climate)-driven changes in the excess ^{234}U flux (Dunk et al., 2002; Henderson, 2002; Robinson et al., 2004a; Robinson et al., 2004b; Esat & Yokoyama, 2010; Chutcharavan et al., 2018). Several studies have proposed that per mil deviations from modern ocean $\delta^{234}\text{U}$ values observed in fossil corals during the last glacial maximum reflect sea-level control on the excess ^{234}U flux (Esat & Yokoyama, 2006, 2010; Chutcharavan et al., 2018). The observed 4–8 ‰ decrease in glacial seawater $\delta^{234}\text{U}$ values is suspected to represent a reduction in continental runoff or the oxidation and release of U stored in interglacial deposits of U from the reducing environment of, for example, mangrove forests. A recent study further revealed elevated $\delta^{234}\text{U}$ in relation to an Antarctic meltwater plume (Li et al., 2023). Nevertheless, the reconstruction of past $\delta^{234}\text{U}$ values can be hampered by subaerial coral diagenesis (Scholz et al., 2004; Frank et al., 2006) or U-series open system behaviour caused by the recoil process of coral embedded sediment (Henderson et al., 1993; Gallup et al., 1994; Henderson & Slowey, 2000; Thompson et al., 2003; Villemant & Feuillet, 2003; Frank et al., 2006). Tropical surface-dwelling corals are always situated in shelf environments, with potential influences of U contributions from local river discharge, submarine groundwater releases, or even the distant transport of freshwater from larger river systems.

Consequently, by examining postmodern, well-preserved and annually-resolved corals, the oceanic U isotopic composition can be investigated to identify any potential systematic local or regional disturbances from freshwater fluxes through rivers and submarine groundwater. To detect subtle changes in oceanic and coral U isotopic compositions, multicollector inductively coupled plasma source mass spectrometry (MC-ICP-MS) is a well-established precise instrumentation for isotopes, that offers external reproducibility better than 1 ‰. Thus, we evaluated the external precision of such measurements via a recently

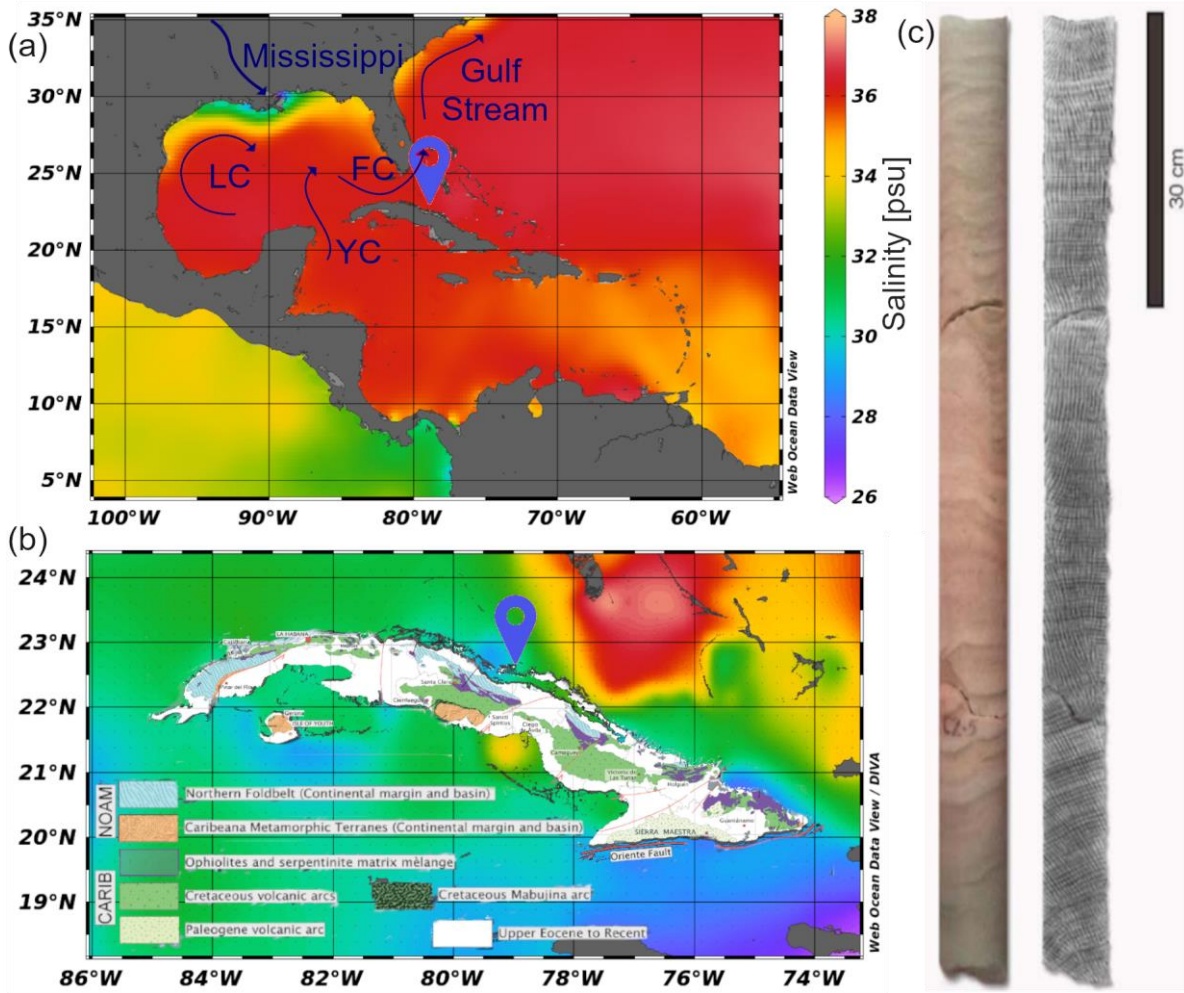
published semi-static data acquisition by Kerber et al. (2023). An external reproducibility of 0.55 ‰ ($2 \sigma_M$) was achieved on seawater and modern aragonitic coral fragments.

To assess the potential impact of shelf water processes on the U isotopic composition of tropical corals and to reveal the potential of U isotopes as freshwater tracer, we selected a long-lived *Orbicella faveolata* coral colony in the western tropical North Atlantic, for which both regional freshwater releases and distant freshwater influence, such as advective transport from the Mississippi River seemed plausible. The tropical Atlantic Ocean is an ideal location for testing potential links between $\delta^{234}\text{U}$ and hydrological and oceanographic conditions at the sub-centennial scale. The northern Caribbean is part of the Atlantic Warm Pool (AWP), which is defined by the sea surface temperature (SST) isotherm exceeding 28.5 °C, which forms each year during early summer (June) and extends into the Gulf of Mexico and the western tropical North Atlantic as summer progresses (July-October) (Wang & Enfield, 2001; Wang et al., 2008). In relation to the AWP and the Intertropical Convergence Zone (ITCZ), the Caribbean hydroclimate is characterized by a wet season from April to October (Martinez et al., 2019), during which hurricanes are also commonly observed (Terry & Kim, 2015). Especially for the Little Ice Age (LIA), which spanned from approximately 1400–1850 (Hodell et al., 2005), substantial changes in the Caribbean SST hydroclimate and potential oceanic circulation have been reconstructed (Haug et al., 2001; Hodell et al., 2005; Richey et al., 2009; Johnson, 2011; Kennett et al., 2012; Fensterer et al., 2013; DeLong et al., 2014; Burn et al., 2016). Consequently, through the study of annual excess ^{234}U variability along a coral core drilled in a colony located at the north of Cuba, we aimed to qualitatively resolve freshwater fluxes into the Gulf of Mexico since the LIA.

2 Material and Methods

2.1 Coral location

For this study, we investigated a coral drill core (CSM-1), 97 cm in length, that was collected in March 2016 from the Sabana Camaguey Archipelago, northern Cuba, approximately 20 km from the main island (Fig. 1) (Alonso-Hernández et al., 2022). The core was obtained from a scleractinian coral colony of the genus *Orbicella faveolata* located at approximately 10 m depth in the Cayo Santa María area (79.10 W, 22.66 N). The core was dated via sclerochronology on the basis of radiographic density images, revealing an age of 237 years, ranging from 1778 to 2015 (Alonso-Hernández et al., 2022). The method has an approximate ± 1 yr uncertainty, which may increase progressively with depth from the top of the coral core (Buddemeier et al., 1974). Additionally, the coral exhibited green growth bands with high Mg contents, possibly due to the incorporation of relatively high levels of organic material into the coral skeleton (Cuny-Guirriec et al., 2019; Alonso-Hernández et al., 2022).



95 **Figure 1: (a) Caribbean annual sea surface salinity with the location of the selected coral core on the northern shore of Cuba, directly**
influenced by the Florida Current (FC) travelling eastwards from Yucatan Current (YC) and the Gulf of Mexico forming the Gulf
Stream. The Loop Current (LC) carries the less saline Mississippi water towards the coral. (b) Annual sea surface salinity off the
coast of Cuba; less salinity is observed at the core location due to terrestrial runoff. With generalized geologic-tectonic map of Cuba
modified from (Iturralde-Vinent et al., 2016) (c) X-ray image of the slab used in the optical densitometry analysis and photograph
100 **of the analysed core (CSM-1) with visible green banding.**

The climate of the region is influenced by the southwestern edge of the high-pressure system over the Atlantic (Fig. S1). The summer and fall seasons correspond to the rainy season with occasional extreme events, such as hurricanes. Hurricanes typically track west- and northwards approximately once every 20 years, affecting mainly the southeast coast of Cuba (Limia et al., 2003; Terry & Kim, 2015). During the winter season, the hydroclimate tends to be dry, with precipitation rates decreasing
105 from 250 mm per month in summer to as low as 25 mm per month in winter (Vose et al., 1992).

The location of the sample core lies within the Florida Strait (Fig. 1), serving as the outflow path for water masses from the Gulf of Mexico, with an estimated flow rate of 28 Sv (Leaman et al., 1995). As a result, the coral is influenced primarily by

waters originating from the Caribbean and Gulf of Mexico, as well as very local continental runoff from the northern part of Cuba and eutrophic waters from mangroves bordering the southern key. An additional major yet distant source of freshwater, the Mississippi River, is located approximately 2,500 km away, but its flood plumes can extend hundreds of kilometres into the Atlantic (Hitchcock et al., 1997). This large North American river has an annual discharge rate of 0.015 Sv, which can increase fivefold during major flood events. In addition, the Mississippi carries large volumes of sediment particles, which have halved during the past century due to the creation of dams (Folwell, 1921; Carroll, 1990). The mean $\delta^{234}\text{U}$ value of the Mississippi waters was assessed to be $335 \text{‰} \pm 110 \text{‰}$, including strong seasonal variability (Grzymko et al., 2007).

115 2.2 Sampling treatment and U extraction

The separation of uranium from the sample carbonate matrix followed the protocol established by Wefing et al. (2017), with modifications outlined by Kerber et al. (2023). Approximately 50–100 mg of the skeletal aragonite sample underwent ultrasonic cleaning and subsequent dissolution in 7 N HNO_3 . To serve as a concentration reference, 100 μl of TriSpike, a mixture containing the synthetic isotopes ^{233}U , ^{236}U and ^{229}Th , was added. Next, uranium was purified through ion exchange chemistry via U/TEVA resin. To remove Ca and other matrix elements, 300 μl U/TEVA chromatographic ion exchange columns were rinsed three times with 7 N HNO_3 . Uranium was then eluted using 3 N and 1 N HCl successively (Horwitz et al., 1992). The sample was dried and redissolved, and the column purification was repeated until the Ca concentration of the final solution was <10 ppm. For MC-ICP-MS measurements, the final uranium fraction was evaporated and dissolved in 1.2 ml of 1 % HNO_3 + 0.05 % HF, with any particulates removed by centrifugation.

125 2.3 MC-ICP-MS measurement

Measurements were conducted at the Institute of Environmental Physics in Heidelberg using a multicollector ICP-MS (ThermoFisher Neptune^{plus}) coupled with an ARIDUS II desolvating nebulizer system and an ESI-SC autosampler. The cup configurations and mounted amplifiers used, as well as the data treatment protocols, are presented in detail in Kerber et al. (2023).

130 Measurements were conducted via the standard bracketing method with the Harwell-Uraninite 1 (HU-1) standard to ensure measurement stability and correct for machine drift. HU-1 was used as an internal bracketing standard for instrumental normalization, its measured $^{234}\text{U}/^{238}\text{U}$ ratio was fixed to a constant reference value during data reduction. This step serves purely as an instrumental correction and does not imply a physical assumption of secular equilibrium. Data evaluation was performed using a Python script for Th/U dating analysis based on Kerber et al. (2025). This script encompasses instrumental background corrections, identification and correction of signal outliers, and adjustment for mass bias, accounting for hydride formation, and addressing tailing and scattering of ^{238}U . ~~Additionally, the data were normalized to the HU-1 standard, operating under the assumption of secular equilibrium.~~ $\delta^{234}\text{U}$ was calculated via the processed activity ratio of $^{234}\text{U}/^{238}\text{U}$ and is expressed in per mil (‰) using the following equation (1).

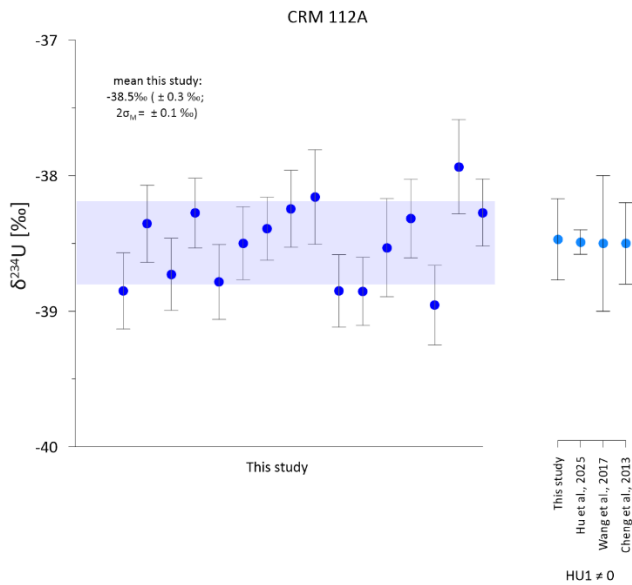
$$140 \quad \delta^{234}\text{U} (\text{‰}) = \left(\frac{A_{234}\text{U}}{A_{238}\text{U}} - 1 \right) \cdot 1000 \quad (1)$$

with decay constants of $\lambda_{238} = 1.55125 \cdot 10^{-10}$ (Jaffey et al., 1971) and $\lambda_{234} = 2.82206 \cdot 10^{-6}$ (Cheng et al., 2013). ~~This places the data on an activity-based scale defined by the adopted decay constants.~~ Internal errors were determined as 2σ from each measurement, whereas external errors were determined through repeated measurements of the NBS-CRM-112A (CRM112A) standard and an in-house seawater standard. ~~Interlaboratory comparison of the $\delta^{234}\text{U}$ values was achieved by continuous measurements of the CRM112A standard and HU-1 as a presumed secular equilibrium standard (Fig. 2). Owing to the observed offset between the certificate value of CRM-112A and its relative value to HU-1, renormalization was necessary; this involved applying the offset of CRM-112A from its certificate value of -1.20‰ (Cheng et al., 2013) to the $\delta^{234}\text{U}$ (HU-1) normalized data (Fig. 2). All the results are provided for consistency with other works normalized to HU-1 $\neq 0$, as suggested by (Chutcharavan et al., 2018) and (Kipp et al., 2022).~~

150 3 Results

3.1 Accuracy

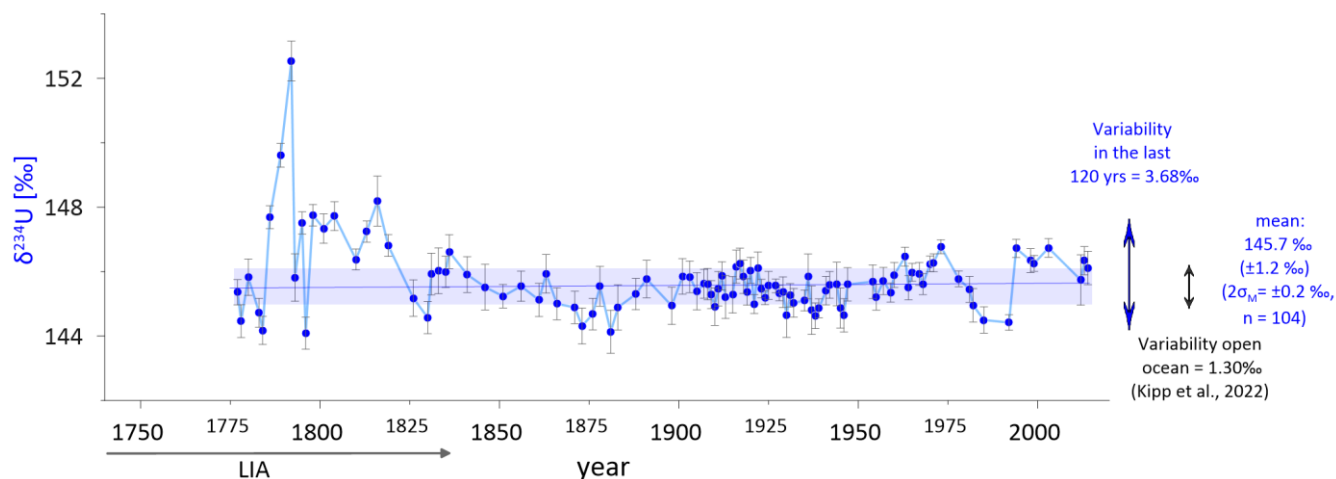
The combined procedural replicates yielded a mean variability of 0.35‰ , with a 2σ reproducibility of 0.54‰ ($n = 6$) in $\delta^{234}\text{U}$ values across replicate groups. The standard deviation from the in-house seawater standard also falls into that range at 0.55‰ (2σ , $n = 11$). The external error was determined by repeated measurements of NBS-CRM-112A in each measurement batch. ~~Accuracy was ensured by comparing these results with studies that have reported relative differences between CRM112A and HU-1 (Robinson et al., 2002; Shen et al., 2002; Deschamps et al., 2003; Andersen et al., 2004; Fietzke et al., 2005; Andersen et al., 2010). Owing to known relative differences, we opted to renormalize our results for CRM112A, which were corrected with the presumption HU-1 = 0 to HU-1 $\neq 0$ by subtracting 1.20‰ for consistency with other studies (Fig. 2). The analyses resulted in a renormalisation of the mean value of $\delta^{234}\text{U}$ (CRM112A) to -38.4812‰ ($\pm 0.3029 \text{‰}$, $2\sigma_M = \pm 0.17 \text{‰}$, $n = 16$).~~ Figure 2 shows the $\delta^{234}\text{U}$ values of CRM112A ~~as measured by several studies normalized to a HU1 value of -1.20‰ . These studies obtained $\delta^{234}\text{U}$ values of $-38.3 \pm 1 \text{‰}$ to $-37.6 \pm 0.8 \text{‰}$ (Cheng et al., 2000; Delanghe et al., 2002; Robinson et al., 2002; Shen et al., 2002; Deschamps et al., 2003; Andersen et al., 2004; Cheng et al., 2013; Pourmand et al., 2014; Wang et al., 2017). Our 16 measurements of CRM112A reveal a mean value of $-38.12 \text{‰} \pm 0.29 \text{‰}$ (2σ). Further advances in coral $\delta^{234}\text{U}$ measurements are described in Greve et al. (in prep.).~~ ~~The small 2σ error compared with what is reported in previous studies (Cheng et al., 2000; Delanghe et al., 2002; Robinson et al., 2002; Shen et al., 2002; Deschamps et al., 2003; Wang et al., 2017; Hu et al., 2025) is attributed to recent advances in data treatment (Kerber et al., 2023; Kerber et al., 2025).~~



170 **Figure 2: The CRM112A standard was repeatedly measured via the bracketing method with the HU-1 standard = -1.2 ‰. The measured. The mean value of -38.512 ‰ ± 0.329 ‰ is in line with other studies normalized to HU1 = -1.2 ‰ (Cheng et al., 2013; Wang et al., 2017; Hu et al., 2025) and is comparable with studies that normalise to HU-1 = 0 if the offset of +1.2 ‰ is applied (Cheng et al., 2000; Delanghe et al., 2002; Robinson et al., 2002; Shen et al., 2002; Deschamps et al., 2003; Andersen et al., 2004).**

3.2 Coral samples

175 Figure 3 shows a total of 104 samples that were collected from the 237-year record of the coral, with each sample representing an integration of one year. These annual samples present a mean $\delta^{234}\text{U}$ value of 145.7558 ‰, with a standard deviation of 1.22 ‰. The large data ensemble and small variance contribute to an uncertainty in the mean value of ± 0.24 ‰ ($2\sigma_M$, $n = 104$). This uncertainty of the mean is comparable to that obtained for the CRM112A standard (Fig. 2). The measured mean $\delta^{234}\text{U}$ value of 145.5875 ‰ is identical to that of modern seawater (Kipp et al., 2022). Analysis of the small-scale variability within the last 165 years from 1850–2014 reveals a range of 3.32 ‰, from 144.3518 ‰ to 147.2750 ‰. This variance is 2.5 times greater than that observed in modern seawater (Kipp et al., 2022). Notably, an even higher variability is observed in earlier 180 years, specifically from 1778–1846, during which the $\delta^{234}\text{U}$ values exhibit a total variance of 8.10 ‰, fluctuating from 143.1740 ‰ to 151.2750 ‰.



185 **Figure 3: Annual $\delta^{234}\text{U}$ measurements ($n = 104$) of a 237-year-old coral. The mean of 145.7558 ‰ ($\pm 0.24 \text{ ‰}$) is identical to the open ocean value of 145.55 ‰ ($\pm 0.28 \text{ ‰}$) (Kipp et al., 2022). The largest deviations from 143.1740 ‰ to 151.2750 ‰ were observed from 1778–1846 at the end of the Little Ice Age (LIA), with the peak value occurring in 1792. The variability in the coral $\delta^{234}\text{U}$ over the last 165 years is approximately 2.5 times greater than the variance expected from observations in the open ocean (Kipp et al., 2022).**

4 Discussion

4.1 Seawater $\delta^{234}\text{U}$ from coral aragonite

190 Corals incorporate the uranium isotopic ratio of seawater ($\delta^{234}\text{U}_{\text{SW}}$) into their skeleton without measurable fractionation (Robinson et al., 2004b; Wang et al., 2017; Kipp et al., 2022). However, one known factor that can cause fractionation is the postdepositional diagenetic alteration of the coral skeletal material (Delanghe et al., 2002; Robinson et al., 2004b; Wang et al., 2017).

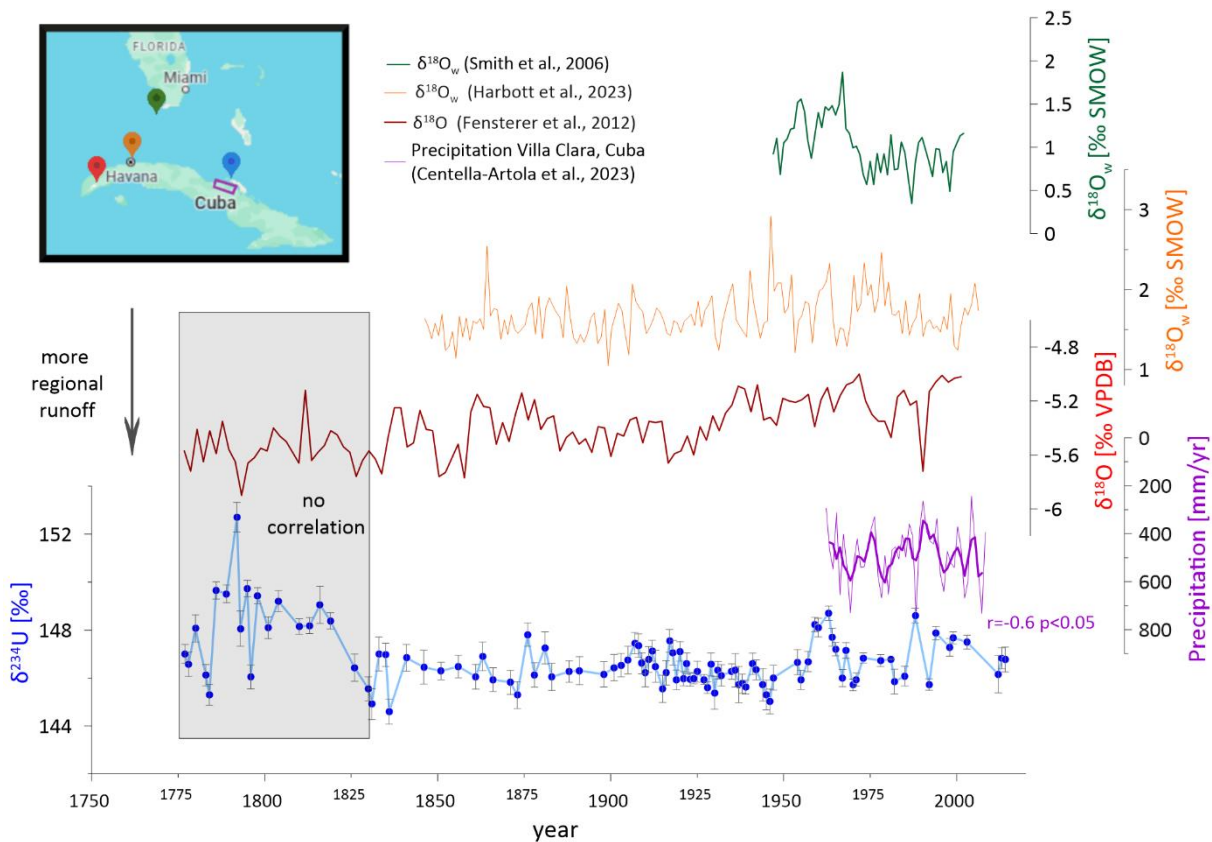
195 Uranium isotope variations in the Cuban coral are independent of growth parameters (e.g., density) or green banding with high Mg concentration (Fig. S3) (Alonso-Hernández et al., 2022). As Mg/Ca is the proxy most sensitive to skeleton diagenesis, such as calcite or secondary aragonite formation (Allison et al., 2007; Hathorne et al., 2011), the absence of correlation between $\delta^{234}\text{U}$ and Mg/Ca suggests that diagenesis has not influenced the $\delta^{234}\text{U}$ values along the core. Studies have shown that secondary aragonite also has a higher U content than primary skeletal aragonite does (Eggins et al., 2005; Allison et al., 2007; Hathorne et al., 2011), which implies a possible correlation between uranium content and isotopic composition. This correlation was not detected in our results (Table S1 and Fig. S3). Furthermore, a diagenetic overprint could result in
 200 extraordinarily high $\delta^{234}\text{U}$ values exceeding 10 ‰ above those of seawater. According to Chutcharavan et al. (2018), a benchmark of 156 ‰ is used to indicate diagenetic alteration of fossil coral material. However, in the coral analysed here, no such elevated values were observed. Consequently, these observations, as well as the excellent agreement of the mean isotopic compositions of corals with those of modern seawater, allow us to conclude that the CSM-1 coral can be used to monitor the U isotopic compositions of local seawater over the past 237 years.

205 Studies conducted in restricted ocean basins have demonstrated a $\delta^{234}\text{U}$ offset towards higher values, a shift attributed to the substantial influence of meltwater or river discharge (Andersen et al., 2007; Zhou et al., 2015; Wang et al., 2017; Arendt et al., 2018). Despite the Caribbean being a semi-enclosed basin, it receives a high inflow rate of Atlantic waters, estimated at 28 Sv, which exit the Caribbean and Gulf of Mexico near the sample location (Johns et al., 2002). These substantial throughflow rates support the strong control of seawater on the coral mean $\delta^{234}\text{U}$ values.

210 **4.2 Coral $\delta^{234}\text{U}$ values as a proxy for hydrological variation**

With excellent reproducibility and overall high precision, even subtle variability can be resolved. The variability in seawater $\delta^{234}\text{U}_{\text{sw}}$ was recently reported to be 1.3 ‰ (Kipp et al., 2022). Under different climate and global weathering conditions, such as during the last sea level low stand and maximum global ice volume, i.e., the Last Glacial Maximum, seawater $\delta^{234}\text{U}_{\text{sw}}$ decreased systematically worldwide by 6 ± 2 ‰ (Henderson, 2002; Esat & Yokoyama, 2006; Chutcharavan et al., 2018). The major sources of isotopic variability in the surface ocean are continental runoff and submerged groundwater. Continental freshwater has a very large range of $\delta^{234}\text{U}$ values from as low as 70 ‰ to 1030 ‰, depending on the continental U cycle driven by erosion and the type of regional weathering (Dunk et al., 2002; Li et al., 2018). In the tropics, chemical weathering prevails, reducing the excess leaching of ^{234}U from the host rock. Moreover, the residence times of freshwater in karstic environments, such as in the Cuban core location, are within days or months to years, resulting in $\delta^{234}\text{U}$ values that are at the lower end of the freshwater scale (Dunk et al., 2002; Paces et al., 2002; Gonzalez-De Zayas et al., 2013; Iturralde-Vinent et al., 2016). Thus, changes in the local freshwater contribution to the ocean could cause the $\delta^{234}\text{U}_{\text{sw}}$ values to shift slightly lower than those of seawater. The annual precipitation from 1960 – 2008 near the coral location has a mean of 482.9 mm yr⁻¹ and varies by approximately 124.5 mm yr⁻¹ (Centella-Artola et al., 2023). Thus, the interannual precipitation variability indicates substantial variations of at least ± 25 % in the local freshwater supply.

225 Over the past 120 years, the coral record has shown considerable variability on decadal timescales, which is approximately 2–3 times greater than that expected in open ocean seawater (Fig. 3) (Andersen et al., 2010; Kipp et al., 2022). Interestingly, the $\delta^{234}\text{U}$ variations have exhibited a negative correlation with the regional precipitation record since 1960 ($r = -0.6$ $p < 0.05$, $n = 21$) (Fig. 4) (Centella-Artola et al., 2023).



230 **Figure 4:** The $\delta^{234}\text{U}$ values from the analysed coral in central northern Cuba (blue) are negatively correlated ($r = -0.60, p < 0.05$) with
 a precipitation record from the same region, starting in 1960 (purple; inverted y-axis) (Centella-Artola et al., 2023). Similar patterns
 are observed with $\delta^{18}\text{O}_w$ values calculated from corals from southern Florida (green) (Smith et al., 2006) and northern Cuba (orange)
 (Harbott et al., 2023), with high $\delta^{234}\text{U}$ values corresponding to high $\delta^{18}\text{O}_w$ values. Additionally, since 1860, there has been a similar
 235 trend in the $\delta^{18}\text{O}$ values from a stalagmite in northwestern Cuba, which are interpreted as a precipitation indicator (red) (Fensterer
 et al., 2012). These alignments show a visible influence of precipitation on the $\delta^{234}\text{U}$ values of the coastal waters in which the coral
 lived, with low $\delta^{234}\text{U}$ values representing greater runoff influences. In the period from 1778–1860, there appears to be no such trend
 between the stalagmite record and the coral record, likely indicating a substantial marine influence on the coral during the end of
 the Little Ice Age.

These subtle variations in $\delta^{234}\text{U}$ are close to the reproducibility limit of the U isotope measurements but are still statistically
 240 noteworthy. The local $\delta^{234}\text{U}_{\text{SW}}$ value is dependent on the input of terrestrial sourced freshwater, such as river runoff and
 submarine groundwater discharge. In Cuba, the residence time of precipitated water is relatively short and in the range of days
 to months due to the karstic terrain (Gonzalez-De Zayas et al., 2013; Iturralde-Vinent et al., 2016). Uranium isotopic
 compositions in groundwater are influenced by both redox conditions and uranium concentrations. Typically, an inverse
 relationship exists between groundwater uranium concentration and $\delta^{234}\text{U}$; deep, reducing groundwaters with low uranium
 245 concentrations tend to show higher $\delta^{234}\text{U}$ values than oxic, near-surface waters with higher concentrations (Osmond & Cowart,
 1976; Asikainen, 1981). Redox conditions also influence uranium mobility and isotope fractionation, with well-oxidizing
 groundwaters yielding lower activity ratios (Suksi et al., 2006). Catchment-scale denudation further affects these ratios: a U-

shaped relationship has been observed, where both low and high denudation rates correspond to elevated $\delta^{234}\text{U}$ values, while intermediate rates yield lower values (Li et al., 2018). Studies from the Yucatán Peninsula and Tampa Bay, Florida, have reported low $\delta^{234}\text{U}$ values in groundwater and estuarine waters, which also showed relatively high uranium concentrations (Osmond & Cowart, 2000; Swarzenski & Baskaran, 2007; Schorndorf et al., 2023). The low $\delta^{234}\text{U}$ values in the coral may therefore reflect shallow groundwater runoff influenced by oxidizing conditions and/or moderate denudation rates in riverine waters in the region. Hence, the freshwater runoff coming from the Carbonate Hinterland (Iturralde-Vinent et al., 2016) and related to precipitation may lead to a moderate decrease of $\delta^{234}\text{U}$ values in coastal seawater. This process likely explains the anticorrelation of coral $\delta^{234}\text{U}$ values, where lower $\delta^{234}\text{U}$ values coincided with high annual precipitation over the last 50 years (Fig. 4). A study of a sediment core situated approximately 100 km east of the analysed coral core revealed a freshwater influence on organic matter by approximately 15 % from 1900–1970 (Alonso-Hernández et al., 2022). During this time, the coral exhibited a mean $\delta^{234}\text{U}$ of 145.25 ‰, at the lower limit of open ocean seawater, possibly reflecting a persistent but minor local freshwater influence. The influence on $\delta^{234}\text{U}$ is likely far lower than that observed for organic matter by Alonso-Hernández et al. (2020) because of the lack of high-discharge rivers nearby.

A commonly used proxy for sea surface salinity is stable oxygen isotopes in seawater ($\delta^{18}\text{O}_{\text{sw}}$), as they depend on both freshwater influx and evaporation (Leder et al., 1996; Gagan et al., 1998; Gagan et al., 2000; Ren et al., 2003). A comparison with reconstructed $\delta^{18}\text{O}_{\text{sw}}$ values from tropical corals in proximity to the sample location also revealed similarities at annual time scales (Fig. 4) (Table S2) (Smith et al., 2006; Harbott et al., 2023). The $\delta^{18}\text{O}_{\text{sw}}$ is calculated from the measured coral $\delta^{18}\text{O}$ values (Smith et al., 2006), which are influenced by seawater $\delta^{18}\text{O}_{\text{sw}}$ and temperature. By subtracting the temperature component derived from the Sr/Ca record of the same coral, the $\delta^{18}\text{O}_{\text{sw}}$ at the time of coral growth can be calculated (Ren et al., 2003). Note that the SST, estimated via the Li/Ca ratio (Alonso-Hernández et al., 2022), is not significantly correlated with the coral $\delta^{234}\text{U}$ values (Fig. S2).

For the 19th century, the coral $\delta^{234}\text{U}$ values aligned with the $\delta^{18}\text{O}$ record of a stalagmite from western Cuba, interpreted as a proxy for rainfall amount (Fensterer et al., 2012). This alignment falls within the uncertainty of the stalagmite age model (Fig. 4). Before 1860, the stalagmite and coral records diverged from one another, suggesting a potential additional source of $\delta^{234}\text{U}$ and its variability. Here, we propose that this source is linked to distant freshwater discharge from the North American continent and/or a synchronous reduction in the strength of the Gulf of Mexico current, which is not traced by the hydroclimate record of the stalagmite.

275 4.3 Variability during the LIA

The highest variability in the coral $\delta^{234}\text{U}$ values occurred between 1778 and 1846, with $\delta^{234}\text{U}$ values ranging from ~~144.1~~~~143.40~~‰ to ~~151.50~~~~152.5~~‰. This time interval of high $\delta^{234}\text{U}$ variability coincides with the end of a period of colder SSTs in the Caribbean during the LIA (Winter et al., 2000; Haase-Schramm et al., 2003; Kilbourne et al., 2008).

4.3.1 Fast and high local runoff

280 Some studies inferred reduced precipitation during the LIA, including Haug et al. (2001) for the southern Caribbean, Hodell et al. (2005) for the Yucatan Peninsula and Richey et al. (2009) for the Gulf of Mexico. However, other studies have reported highly variable amounts of rainfall in the northern part of the Caribbean and the Gulf of Mexico (Kennett et al., 2012; Fensterer et al., 2013; DeLong et al., 2014; Burn et al., 2016). Historical records in Cuba also documented periods of drought interspersed with several severe hurricanes in the late 1700s (Johnson, 2011) (Fig. 5). A high amount of local precipitation with fast
285 discharge rates can explain the low $\delta^{234}\text{U}$ values recorded in the coral, as discussed above. The punctuated low values recorded by the coral suggest multiple local extreme precipitation events, particularly from 1778–1847 (Fig. 5). Wang and Enfield (2001) reported that an extended Atlantic Warm Pool fuels precipitation and the frequency of more intense tropical storms. Additionally, DeLong et al. (2014) linked fluctuating SSTs in Dry Tortugas and Puerto Rico (Kilbourne et al., 2008) to a variability in the size of the western hemispheric warm pool. The reconstructed SST from the Li/Ca in the analysed coral also
290 exhibited high variability during that time (Alonso-Hernández et al., 2022). Therefore, fluctuating $\delta^{234}\text{U}$ values further support times of fast and high local runoff.

Another possible influence on the $\delta^{234}\text{U}$ values is land use change on the Cuban island. Beginning around 1820, widespread deforestation was undertaken to expand sugarcane cultivation (Monzote, 2008). This deforestation likely increased soil erosion and enhanced continuous runoff into coastal waters (Monzote, 2024). Prior to widespread deforestation, uranium delivery to
295 coastal waters was limited in magnitude and more episodic, as forest cover suppressed soil erosion and regulated hydrological fluxes (Palmer & Edmond, 1993; Zhang et al., 2023). Under these conditions, the isotopic composition of uranium was strongly influenced by local lithological heterogeneity. Inputs derived from shallowly weathered soils would have carried elevated $\delta^{234}\text{U}$ values due to preferential leaching of ^{234}U , whereas contributions from less-weathered bedrock or carbonate units closer to secular equilibrium could have lowered ^{234}U toward or below the marine mean (Chabaux et al., 2008; Li et al., 2018). The
300 archive therefore records large variability, including excursions to relatively low $\delta^{234}\text{U}$ values, reflecting the sensitivity of the system to short-term and spatially heterogeneous sources.

Following the onset of large-scale deforestation in the early nineteenth century, enhanced and continuous soil erosion generated a greater and more sustained flux of weathering-derived uranium to the coastal environment (Chabaux et al., 2008; Li et al., 2018; Monzote, 2024). Because ^{234}U is preferentially mobilized during chemical weathering, this terrestrial input typically
305 carried $\delta^{234}\text{U}$ values above equilibrium (Chabaux et al., 2008; Li et al., 2018). The larger and more consistent flux buffered the

influence of localized or episodic inputs, leading to a stabilization of $\delta^{234}\text{U}$ values in the archive and their convergence toward the oceanic mean.

310 Figure 5 shows the Ba/Ca record of the coral core, exhibits a positive covariation with the $\delta^{234}\text{U}$ record except for a particular strong Ba/Ca peak surrounding the year 1820 to 1830. The correspondence suggests that both proxies respond to a common environmental driver, potentially linked to changes in terrigenous input or nearshore hydrographic conditions. Periods of enhanced Ba/Ca and $\delta^{234}\text{U}$ broadly coincide with phases of precipitation extremes until 1820, when Ba/Ca decouples from $\delta^{234}\text{U}$. This event coincides with intensified land-use change on Cuba, including widespread deforestation after 1820, which has been shown to increase soil erosion and the export of particulate and dissolved material to the coastal ocean. During the same time interval, precipitation moderately increases as indicated by the speleothem $\delta^{18}\text{O}$ values (Fig. 4). Obviously Ba/Ca response

315 more sensitive to such local vegetation and soil changes that coincide with precipitation changes as compared to $\delta^{234}\text{U}$, which does not reveal a significant increase during those years.

Therefore, the lack of synchronous variability between the coral $\delta^{234}\text{U}$ record and the stalagmite $\delta^{18}\text{O}$ record from Cuba (Fensterer et al., 2012) suggests that local precipitation changes can unlikely explain the observed $\delta^{234}\text{U}$ variability between the years 1780 - 1850. Together, these observations imply that the $\delta^{234}\text{U}$ signal recorded in the coral reflects marine and to a

320 lesser degree regional land-use-related influences rather than a simple response to island-scale rainfall variability.

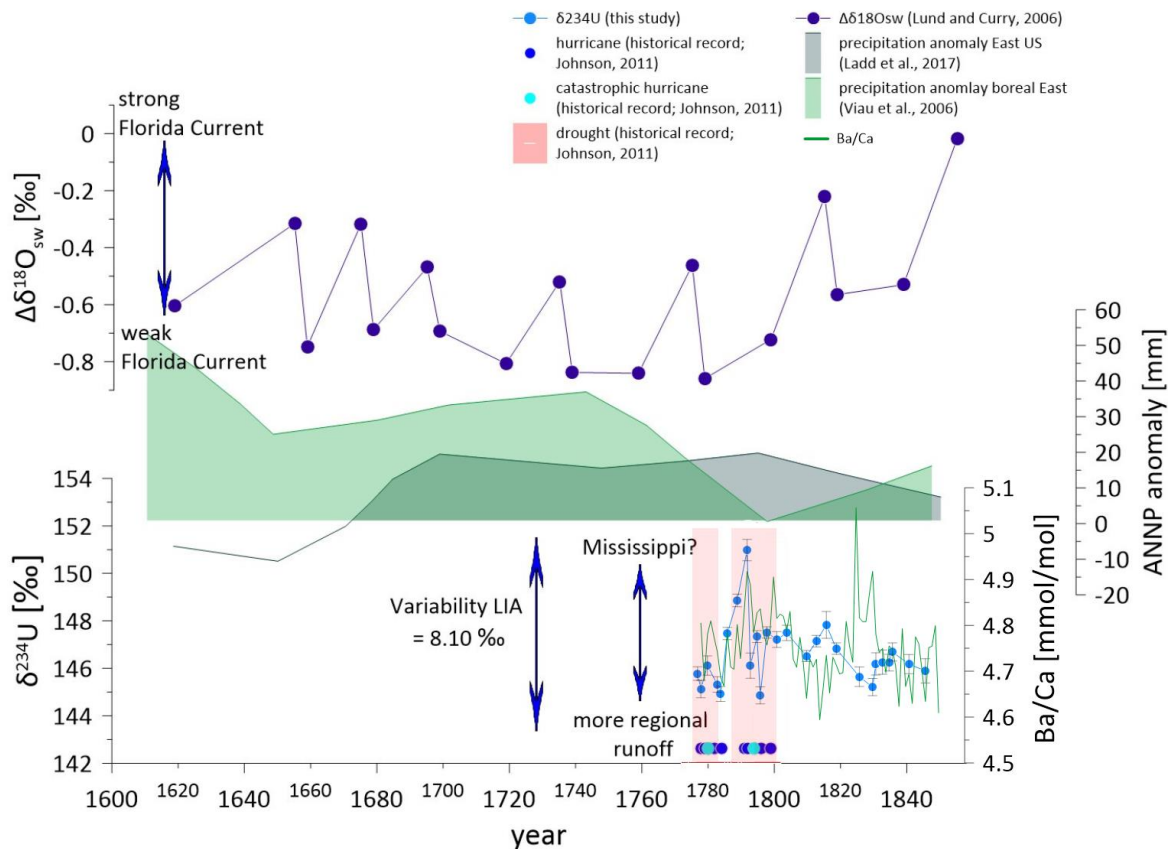


Figure 5: $\delta^{234}\text{U}$ values (blue) from 1778–1850 plotted together with the timing of hydrological events documented in historical records (Johnson, 2011), indicating times of high hydrological fluctuation with droughts (red), hurricanes (dark blue), and catastrophic hurricanes (light blue). **The green line shows Ba/Ca ratios of the coral core corresponding to the $\delta^{234}\text{U}$ values. During these times, the $\delta^{234}\text{U}$ values exhibited high variability, ranging from 143.40 ‰ to 151.50 ‰ in 1792. According to the present age model this high value occurred during a period of recurrent major hurricanes.** Florida Current strength is inferred from $\Delta\delta^{18}\text{O}_{\text{sw}}$ differences between the Gulf of Mexico and the Bahamas Channel (purple; (Lund & Curry, 2006)), where more negative values reflect a weaker current during the LIA. Superimposed precipitation anomalies over eastern North America (dark green; (Ladd et al., 2018)) and the boreal east (light green; (Viau et al., 2006)) show enhanced precipitation during this same interval, consistent with a weakened Florida Current and elevated variability in $\delta^{234}\text{U}$ values.

4.3.2 Possible Mississippi influence

With a smaller warm pool, precipitation over the eastern North American continent has increased due to changes in atmospheric circulation (Wang et al., 2008; Ladd et al., 2018). This enhancement also extended to parts of the Mississippi recharge basin (Ladd et al., 2018), potentially leading to increased runoff. The Mississippi River was found to have elevated $\delta^{234}\text{U}$ values averaging approximately 335 ‰, with strong LIA variations and values reaching up to 450 ‰ (Grzymko et al., 2007). During the end of the LIA, the coral $\delta^{234}\text{U}$ values are frequently elevated by > 3 ‰ compared with those in the mean ocean and are even more significant than those in locally depleted runoff. Thus, we hypothesize that these elevated $\delta^{234}\text{U}$ values

340 resulted from ^{234}U -enriched waters from Mississippi that reached the Gulf of Mexico and induced excess ^{234}U to the coral site. Upon discharge, the river plume is carried westward and southwestward along the Louisiana-Texas shelf within the Gulf's general cyclonic circulation, often described as the Mexican Current system, which flows counter to the eastward Loop Current (Androulidakis & Kourafalou, 2013). Although this circulation pattern tends to retain Mississippi-derived material within the western Gulf, episodic entrainment into the Loop Current has been documented during periods of strong eddy activity or
345 northward Loop Current extensions (Muller-Karger, 2000; Morey et al., 2003; Androulidakis & Kourafalou, 2013). Once incorporated into the Loop Current, dissolved constituents such as uranium could be transported eastward through the Florida Strait and subsequently redistributed in the southern Florida Strait along the northern Cuban shelf (Fratantoni et al., 1998; Androulidakis et al., 2020). Indeed, analysis of satellite salinity measurements indicates, that Mississippi-sourced waters can extend as far as the Florida Straight (Cummings & Smedstad, 2013). Because uranium in seawater is conservative, with a
350 residence time on the order of 400–500 kyr (Jaffey et al., 1971; Chen et al., 1986), inputs from the Mississippi would rapidly mix with the surrounding marine reservoir. While this makes it unlikely that Mississippi-derived uranium dominated the local isotopic budget, periodic variability of the Loop Current or increased fluvial fluxes could have enhanced its relative contribution. Such variability may have contributed to shifts in $\delta^{234}\text{U}$ values at the site, particularly prior to the stabilization associated with nineteenth-century land-use change on Cuba and under differing oceanographic settings.

355 The LIA likely made the Gulf of Mexico-Caribbean system more dynamic and variable. Periods of stronger winds and increased Mississippi River discharge would have enhanced the eastward advection of river water across the northern Gulf and its subsequent entrainment into the Loop Current, favouring export toward the Straits of Florida and the northern Cuban shelf (Muller-Karger, 2000; Morey et al., 2003). At the same time, wind forcing and Caribbean eddies exert strong control over Loop Current extension and eddy shedding, at times shortening the shedding period to 3–7 months or prolonging it to
360 14–16 months (Oey et al., 2003). Thus, while enhanced storminess and runoff during the LIA may have increased the potential for Mississippi River influence on Cuban shelf waters, alternating phases of Loop Current suppression by Caribbean anticyclones would have periodically dampened this transport. Explaining the high variability in the $\delta^{234}\text{U}$ values from the coral during the End of the LIA.

A strong Caribbean current would more efficiently dilute any freshwater signal than a reduced Gulf of Mexico throughflow.
365 During the LIA, Lund et al. (2006) reported a decrease in the throughflow rate at the Florida Strait by approximately 10 %, predominantly in the wind-driven part of the Florida Current. This reduction, coupled with an increase in precipitation over the eastern part of the North American continent (Lund et al., 2006; Ladd et al., 2018), could reasonably account for a higher total U discharge from the Mississippi River. This scenario likely contributed to the observed punctuated increase in $\delta^{234}\text{U}$ values of 2–3 ‰ during the LIA. Lund and Curry (2006) and Richey et al. (2009) further suggested saltier conditions in the
370 Gulf of Mexico during the LIA, bringing the Caribbean Basin closer to today's conditions of semi-enclosed basins such as the Mediterranean Sea. These basins present elevated $\delta^{234}\text{U}$ values due to restricted access from open ocean seawater, high evaporation rates and the input of much freshwater and submerged groundwater from terrestrial sources (Border, 2020).

However, changes in throughflow of up to 10 % are small overall compared with possible major changes in U runoff and its isotopic composition.

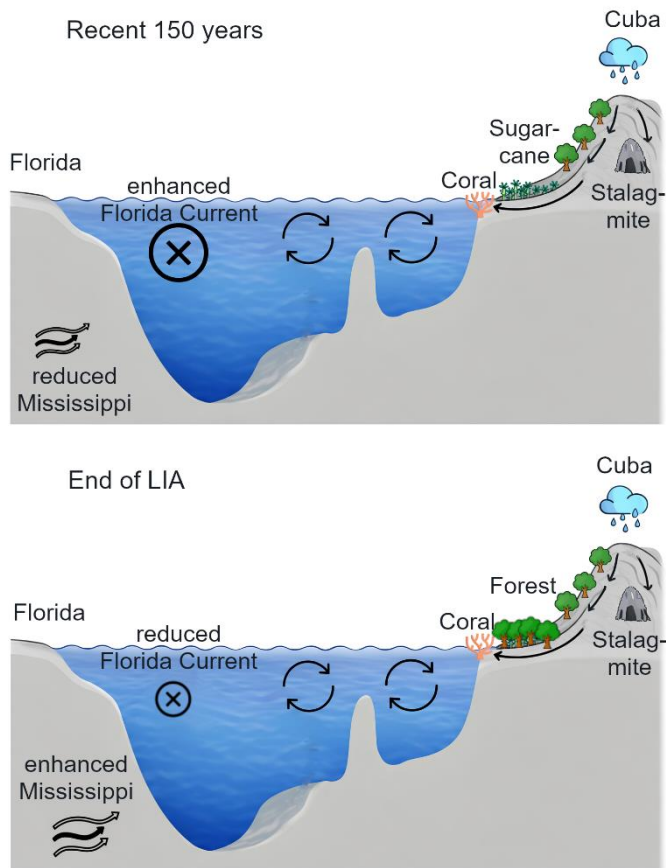
375 Given the capacity for Ba and other trace elements to be transported over large distances within the Gulf of Mexico, enhanced influence of the Mississippi River plume represents a plausible cause for the correlation of Ba/Ca and $\delta^{234}\text{U}$ in the coral core observed at the end of LIA, with the exception of a local induced strong Ba/Ca increase from deforestation over the years 1820 to 1830.

380 This interpretation is consistent with the absence of coherent variability between the coral $\delta^{234}\text{U}$ record and the Cuban stalagmite $\delta^{18}\text{O}$ record (Fensterer et al., 2012), which argues against island-scale precipitation and local runoff as the dominant controls. Instead, the decoupling of these records points toward a stronger role for large-scale river discharge and marine transport processes of U into the Gulf of Mexico as a whole. In this context, increased Mississippi uranium runoff into the Gulf of Mexico during the terminal phase of the LIA, potentially associated with enhanced meltwater and sediment fluxes from higher latitudes, provides a viable explanation for the elevated $\delta^{234}\text{U}$ values observed during this interval.

385 The discussion above assumes that the $\delta^{234}\text{U}$ values in the coral are influenced solely by Mississippi freshwater and seawater, neglecting the potential impact of other sources with different $\delta^{234}\text{U}$ ratios. The reduced wind-driven portion of the Florida Current, which originates from the North Atlantic Subtropical Gyre (Lund et al., 2006), results in a greater contribution of South Atlantic sourced water, potentially affecting the coral $\delta^{234}\text{U}$ ratios. South Atlantic waters are further influenced by the significant discharge of the Amazon and Orinoco rivers near the entrance of the Caribbean (Vorosmarty et al., 1998; Paterne et al., 2023). The Amazon River has elevated $\delta^{234}\text{U}$ values of 204 ‰ (± 4 ‰) (Swarzenski et al., 2004; Border, 2020). However, a study of uranium concentrations and $\delta^{234}\text{U}$ values in the Amazon delta identified an uranium sink due to anaerobic conditions

390 (Border, 2020), suggesting that Amazon-derived uranium does not have a significant large-scale influence on Cuban corals. Changes in Florida Current strength may have influenced the residence time of river-derived signals within the Gulf of Mexico. However, circulation changes alone are unlikely to generate the observed elevation in $\delta^{234}\text{U}$ values without the presence of a
395 high- $\delta^{234}\text{U}$ freshwater endmember. The Mississippi River represents such a source of isotopically enriched uranium injected into the Gulf of Mexico and its variability is consistent with the observed covariance between Ba/Ca and $\delta^{234}\text{U}$ in the coral record. Taken together, the available constraints are most consistent with enhanced Mississippi discharge as a principal contributor to the late LIA $\delta^{234}\text{U}$ variability, with circulation changes influencing the magnitude and expression of the signal. These changes end around the year 1820, when global temperatures start increasing. Between 1820 to 1830 rapid local
400 deforestation of the Cuba Island caused a pulse of Ba runoff to the ocean.

-Further spatially resolved $\delta^{234}\text{U}$ records, particularly from sites proximal to the Mississippi River mouth such as Flower Garden Banks (DeLong et al., 2023), would allow quantitative evaluation of the predicted fluvial gradient and help constrain the relative contributions of discharge versus circulation changes. Additional groundwater characterization and broader Caribbean coral records would refine the regional hydrographic context of the late LIA variability.



405

Figure 6: Schematic comparison of environmental conditions during the end of the Little Ice Age (LIA) and the last ~150 years. The lower panel depicts the terminal LIA, characterized by enhanced Mississippi River discharge, reduced Florida Current strength, and predominantly forested land cover in Cuba. The upper panel represents the recent period, with reduced Mississippi influence, strengthened Florida Current transport, and expanded agricultural land use in Cuba. Arrows indicate relative changes in river input, ocean circulation, and terrestrial runoff pathways affecting the coral site north of Cuba.

410

5 Conclusion

This study presents the first annually resolved coral $\delta^{234}\text{U}$ record spanning a 237-year-long record of seawater $\delta^{234}\text{U}$ from the northern part of Cuba, which was obtained via analysis of the uranium isotopic composition along a coral core of *Orbicella faveolata*. Our results confirm that coral $\delta^{234}\text{U}$ reliably records the seawater composition ($\delta^{234}\text{U}_{\text{SW}}$) without significant diagenetic alteration, as evidenced by the lack of correlation between $\delta^{234}\text{U}$, density and Mg/Ca ratios. The coral has a mean $\delta^{234}\text{U}$ value of 145.7453 ‰ (± 0.21 ‰), which is identical to the open ocean value of 145.55 ‰ (± 0.28 ‰). Decadal $\delta^{234}\text{U}$ variations are approximately 2–3 times greater than those in open ocean seawater and correlate inversely with regional

415

precipitation since 1960 ($r = -0.6$, $p < 0.05$), suggesting an influence of local terrestrial freshwater input, likely from surface runoff and submerged groundwaters. From 1778–1846, coinciding with the end of the Little Ice Age, the $\delta^{234}\text{U}$ record exhibited high variability, with values ranging from 143.40 ‰ to 151.50 ‰, which suggests substantial hydrological changes characterized by severe droughts and increased hurricane activity. Changes in atmospheric circulation during that time also led to increased precipitation over the eastern North American continent, including the Mississippi drainage basin. Thus, elevated $\delta^{234}\text{U}$ values are potentially related to stronger winds and increased freshwater input from the Mississippi River, and reduced throughflow in the Florida Strait, which have enhanced the potential for river water to reach the northern Cuban shelf. And caused a 2–3 ‰ increase in coral $\delta^{234}\text{U}$, which a greater variability during the end of the LIA. However, the influence of other far more distant freshwater sources, such as the Amazon River, was likely minimal due to localized uranium sinks. [This study highlights the potential of coral \$\delta^{234}\text{U}\$ as a promising proxy for reconstructing past hydrographic and riverine variability.](#)

Credit authorship contribution statement

430 SG: conceptualization, data production, interpretation and writing
NF: conceptualization, MC-ICPMS support, mentoring, and data quality control
SW: conceptualization, and hydroclimate records from speleothems
PM: sample supply, SST calculation and trace element measurement
ED: trace element measurement
435 CAH: sample supply, SST calculation
MGB: sample supply

Acknowledgements

This research was funded by the Deutsche Forschungsgemeinschaft—Project number 468685637—SPP 2299/Project number 441832482 “Tropical Climate Variability & Coral Reefs” and project number 247825108. We further thank René Eichstädter
440 for analytical support, as well as Athulya Babu and Marius Feuerle for their assistance in the laboratory.

Open research

The raw data of the figures and tables presented in this paper are found in the Supplement and at the PANGAEA open data library (<https://doi.pangaea.de/10.1594/PANGAEA.973159>).

References

445 Allison, N., Finch, A. A., Webster, J. M., & Clague, D. A. (2007). Palaeoenvironmental records from fossil corals: The effects of submarine diagenesis on temperature and climate estimates. *Geochimica et Cosmochimica Acta*, 71(19), 4693-4703. <https://doi.org/10.1016/j.gca.2007.07.026>

- Alonso-Hernández, C. M., Fanelli, E., Diaz-Asencio, M., Santamaría, J. M., & Morera-Gómez, Y. (2020). Carbon and nitrogen isotopes to distinguish sources of sedimentary organic matter in a Caribbean estuary. *Isotopes in Environmental and Health Studies*, 56(5-6), 654-672. <https://doi.org/10.1080/10256016.2020.1819263>
- Alonso-Hernández, C. M., Gómez-Batista, M., Helguera Pedraza, Y., Hernández-Albernas, J., Rico-Esenaro, S. D., Ruiz-Fernández, A. C., Sánchez-Cabeza, J. A., Douville, E., & Montagna, P. (2022). Registro de temperatura superficial del mar (1778-2015) en *Orbicella faveolata* (Cnidaria: Scleractinia) del arrecife Cayo Santa María, Cuba. In (Vol. 42, pp. 37-53): *Revista de Investigaciones Marinas*.
- Andersen, M. B., Elliott, T., Freymuth, H., Sims, K. W., Niu, Y., & Kelley, K. A. (2015). The terrestrial uranium isotope cycle. *Nature*, 517(7534), 356-359. <https://doi.org/10.1038/nature14062>
- Andersen, M. B., Stirling, C. H., Porcelli, D., Halliday, A. N., Andersson, P. S., & Baskaran, M. (2007). The tracing of riverine U in Arctic seawater with very precise $^{234}\text{U}/^{238}\text{U}$ measurements. *Earth and Planetary Science Letters*, 259(1-2), 171-185. <https://doi.org/10.1016/j.epsl.2007.04.051>
- Andersen, M. B., Stirling, C. H., Potter, E. K., & Halliday, A. N. (2004). Toward epsilon levels of measurement precision on $^{234}\text{U}/^{238}\text{U}$ by using MC-ICPMS. *International Journal of Mass Spectrometry*, 237(2), 107-118. <https://doi.org/https://doi.org/10.1016/j.ijms.2004.07.004>
- Andersen, M. B., Stirling, C. H., Zimmermann, B., & Halliday, A. N. (2010). Precise determination of the open ocean $^{234}\text{U}/^{238}\text{U}$ composition. *Geochemistry, Geophysics, Geosystems*, 11(12). <https://doi.org/10.1029/2010gc003318>
- Androulidakis, Y., Kourafalou, V., Le Hénaff, M., Kang, H., Ntaganou, N., & Hu, C. (2020). Gulf Stream evolution through the Straits of Florida: the role of eddies and upwelling near Cuba. *Ocean Dynamics*, 70(8), 1005-1032. <https://doi.org/10.1007/s10236-020-01381-5>
- Androulidakis, Y. S., & Kourafalou, V. H. (2013). On the processes that influence the transport and fate of Mississippi waters under flooding outflow conditions. *Ocean Dynamics*, 63(2), 143-164. <https://doi.org/10.1007/s10236-012-0587-8>
- Arendt, C. A., Aciego, S. M., Sims, K. W. W., Das, S. B., Sheik, C., & Stevenson, E. I. (2018). Influence of glacial meltwater on global seawater $\delta^{234}\text{U}$. *Geochimica et Cosmochimica Acta*, 225, 102-115. <https://doi.org/10.1016/j.gca.2018.01.007>
- Asikainen, M. (1981). State of disequilibrium between ^{238}U , ^{234}U , ^{226}Ra and ^{222}Rn in groundwater from bedrock. *Geochimica et Cosmochimica Acta*, 45(2), 201-206. [https://doi.org/https://doi.org/10.1016/0016-7037\(81\)90163-0](https://doi.org/https://doi.org/10.1016/0016-7037(81)90163-0)
- Border, E. C. (2020). *Variability of $\delta^{234}\text{U}$ in the Mediterranean Sea, Amazon Estuary, and Atlantic Ocean* (Publication Number Available from INIS: http://inis.iaea.org/search/search.aspx?orig_q=RN:52022202; Available from INIS in electronic form. Also available from: <https://d-nb.info/1215758243/34>; Available from: <https://fiz.tind.io/record/335900/files/335900.pdf>)
- Buddemeier, R. W., Maragos, J. E., & Knutson, D. W. (1974). Radiographic studies of reef coral exoskeletons: Rates and patterns of coral growth. *Journal of Experimental Marine Biology and Ecology*, 14(2), 179-199. [https://doi.org/https://doi.org/10.1016/0022-0981\(74\)90024-0](https://doi.org/https://doi.org/10.1016/0022-0981(74)90024-0)
- Burn, M. J., Holmes, J., Kennedy, L. M., Bain, A., Marshall, J. D., & Perdikaris, S. (2016). A sediment-based reconstruction of Caribbean effective precipitation during the ‘Little Ice Age’ from Freshwater Pond, Barbuda. *The Holocene*, 26(8), 1237-1247. <https://doi.org/10.1177/0959683616638418>
- Carroll, J. L. (1990). Dams and Damages: The Ojibway, the United States, and the Mississippi Headwaters Reservoirs. *Minnesota History*, 52(1), 2-15.
- Centella-Artola, A., Bezanilla-Morlot, A., Serrano-Notivoli, R., Vazquez-Montenegro, R., Sierra-Lorenzo, M., & Chang-Dominguez, D. (2023). A new long term gridded daily precipitation dataset at high-resolution for Cuba (CubaPrec1). *Data Brief*, 48, 109294. <https://doi.org/10.1016/j.dib.2023.109294>
- Chabaux, F., Bourdon, B., & Riotte, J. (2008). Chapter 3 U-Series Geochemistry in Weathering Profiles, River Waters and Lakes. In S. Krishnaswami & J. K. Cochran (Eds.), *Radioactivity in the Environment* (Vol. 13, pp. 49-104). Elsevier. [https://doi.org/https://doi.org/10.1016/S1569-4860\(07\)00003-4](https://doi.org/https://doi.org/10.1016/S1569-4860(07)00003-4)
- Chen, J. H., Lawrence Edwards, R., & Wasserburg, G. J. (1986). ^{238}U , ^{234}U and ^{232}Th in seawater. *Earth and Planetary Science Letters*, 80(3), 241-251. [https://doi.org/https://doi.org/10.1016/0012-821X\(86\)90108-1](https://doi.org/https://doi.org/10.1016/0012-821X(86)90108-1)
- Cheng, H., Edwards, R. L., Hoff, J., Gallup, C. D., Richards, D. A., & Asmerom, Y. (2000). The half-lives of uranium-234 and thorium-230. *Chemical Geology*, 169(1), 17-33. [https://doi.org/https://doi.org/10.1016/S0009-2541\(99\)00157-6](https://doi.org/https://doi.org/10.1016/S0009-2541(99)00157-6)

- Cheng, H., Lawrence Edwards, R., Shen, C.-C., Polyak, V. J., Asmerom, Y., Woodhead, J., Hellstrom, J., Wang, Y., Kong, X., Spötl, C., Wang, X., & Calvin Alexander, E. (2013). Improvements in ²³⁰Th dating, ²³⁰Th and ²³⁴U half-life values, and U–Th isotopic measurements by multi-collector inductively coupled plasma mass spectrometry. *Earth and Planetary Science Letters*, 371-372, 82-91. <https://doi.org/10.1016/j.epsl.2013.04.006>
- 500 Chutcharavan, P. M., Dutton, A., & Ellwood, M. J. (2018). Seawater ²³⁴U/²³⁸U recorded by modern and fossil corals. *Geochimica et Cosmochimica Acta*, 224, 1-17. <https://doi.org/10.1016/j.gca.2017.12.017>
- Cummings, J. A., & Smedstad, O. M. (2013). Variational Data Assimilation for the Global Ocean. In S. K. Park & L. Xu (Eds.), *Data Assimilation for Atmospheric, Oceanic and Hydrologic Applications (Vol. II)* (pp. 303-343). Springer Berlin Heidelberg. https://doi.org/10.1007/978-3-642-35088-7_13
- 505 Cuny-Guirriec, K., Douville, E., Reynaud, S., Allemand, D., Bordier, L., Canesi, M., Mazzoli, C., Taviani, M., Canese, S., McCulloch, M., Trotter, J., Rico-Esenaro, S. D., Sanchez-Cabeza, J.-A., Ruiz-Fernández, A. C., Carricart-Ganivet, J. P., Scott, P. M., Sadekov, A., & Montagna, P. (2019). Coral Li/Mg thermometry: Caveats and constraints. *Chemical Geology*, 523, 162-178. <https://doi.org/10.1016/j.chemgeo.2019.03.038>
- 510 Delanghe, D., Bard, E., & Hamelin, B. (2002). New TIMS constraints on the uranium-238 and uranium-234 in seawaters from the main ocean basins and the Mediterranean Sea. *Marine Chemistry*, 80(1), 79-93. [https://doi.org/https://doi.org/10.1016/S0304-4203\(02\)00100-7](https://doi.org/https://doi.org/10.1016/S0304-4203(02)00100-7)
- DeLong, K. L., Flannery, J. A., Poore, R. Z., Quinn, T. M., Maupin, C. R., Lin, K., & Shen, C.-C. (2014). A reconstruction of sea surface temperature variability in the southeastern Gulf of Mexico from 1734 to 2008 C.E. using cross-dated Sr/Ca records from the coral *Siderastrea siderea*. *Paleoceanography*, 29(5), 403-422. <https://doi.org/https://doi.org/10.1002/2013PA002524>
- 515 DeLong, K. L., Palmer, K., Wagner, A. J., Weerabaddana, M. M., Slowey, N., Herrmann, A. D., Duprey, N., Martínez-García, A., Jung, J., Hajdas, I., Rose, N. L., Roberts, S. L., Roberts, L. R., Cundy, A. B., Gaca, P., Milton, J. A., Yang, H., Turner, S. D., Huang, C.-Y., . . . Zinke, J. (2023). The Flower Garden Banks *Siderastrea siderea* coral as a candidate Global boundary Stratotype Section and Point for the Anthropocene series. *The Anthropocene Review*, 10(1), 225-250. <https://doi.org/10.1177/20530196221147616>
- 520 Deschamps, P., Doucelance, R., Ghaleb, B., & Michelot, J.-L. (2003). Further investigations on optimized tail correction and high-precision measurement of uranium isotopic ratios using multi-collector ICP-MS. *Chemical Geology*, 201, 141–160.
- 525 Dunk, R. M., Mills, R. A., & Jenkins, W. J. (2002). A reevaluation of the oceanic uranium budget for the Holocene. *Chemical Geology*, 190(1), 45-67. [https://doi.org/https://doi.org/10.1016/S0009-2541\(02\)00110-9](https://doi.org/https://doi.org/10.1016/S0009-2541(02)00110-9)
- Eggins, S. M., Grün, R., McCulloch, M. T., Pike, A. W. G., Chappell, J., Kinsley, L., Mortimer, G., Shelley, M., Murray-Wallace, C. V., Spötl, C., & Taylor, L. (2005). In situ U-series dating by laser-ablation multi-collector ICPMS: new prospects for Quaternary geochronology. *Quaternary Science Reviews*, 24(23), 2523-2538. <https://doi.org/https://doi.org/10.1016/j.quascirev.2005.07.006>
- 530 Esat, T. M., & Yokoyama, Y. (2006). Variability in the uranium isotopic composition of the oceans over glacial–interglacial timescales. *Geochimica et Cosmochimica Acta*, 70(16), 4140-4150. <https://doi.org/https://doi.org/10.1016/j.gca.2006.06.013>
- 535 Esat, T. M., & Yokoyama, Y. (2010). Coupled uranium isotope and sea-level variations in the oceans. *Geochimica et Cosmochimica Acta*, 74(24), 7008-7020. <https://doi.org/https://doi.org/10.1016/j.gca.2010.09.007>
- Fensterer, C., Scholz, D., Hoffmann, D., Spötl, C., Pajón, J. M., & Mangini, A. (2012). Cuban stalagmite suggests relationship between Caribbean precipitation and the Atlantic Multidecadal Oscillation during the past 1.3 ka. *The Holocene*, 22(12), 1405-1412. <https://doi.org/10.1177/0959683612449759>
- 540 Fensterer, C., Scholz, D., Hoffmann, D. L., Spötl, C., Schröder-Ritzrau, A., Horn, C., Pajón, J. M., & Mangini, A. (2013). Millennial-scale climate variability during the last 12.5ka recorded in a Caribbean speleothem. *Earth and Planetary Science Letters*, 361, 143-151. <https://doi.org/https://doi.org/10.1016/j.epsl.2012.11.019>
- Fietzke, J., Liebetrau, V., Eisenhauer, A., & Dullo, C. (2005). Determination of uranium isotope ratios by multi-static MIC-ICP-MS: method and implementation for precise U- and Th-series isotope measurements. *J. Anal. At. Spectrom.*, 20(5), 395-401.
- 545 Folwell, W. W. (1921). *A History of Minnesota*. Minnesota Historical Society. <https://books.google.de/books?id=2SYUAAAAYAAJ>

- Frank, N., Turpin, L., Cabioch, G., Blamart, D., Tressens-Fedou, M., Colin, C., & Jean-Baptiste, P. (2006). Open system U-series ages of corals from a subsiding reef in New Caledonia: Implications for sea level changes, and subsidence rate. *Earth and Planetary Science Letters*, 249(3), 274-289. <https://doi.org/https://doi.org/10.1016/j.epsl.2006.07.029>
- 550 Fratantoni, P. S., Lee, T. N., Podesta, G. P., & Muller-Karger, F. (1998). The influence of Loop Current perturbations on the formation and evolution of Tortugas eddies in the southern Straits of Florida. *Journal of Geophysical Research: Oceans*, 103(C11), 24759-24779. <https://doi.org/https://doi.org/10.1029/98JC02147>
- Gagan, M. K., Ayliffe, L. K., Beck, J. W., Cole, J. E., Druffel, E. R. M., Dunbar, R. B., & Schrag, D. P. (2000). New views of tropical paleoclimates from corals. *Quaternary Science Reviews*, 19(1), 45-64. [https://doi.org/https://doi.org/10.1016/S0277-3791\(99\)00054-2](https://doi.org/https://doi.org/10.1016/S0277-3791(99)00054-2)
- 555 Gagan, M. K., Ayliffe, L. K., Hopley, D., Cali, J. A., Mortimer, G. E., Chappell, J., McCulloch, M. T., & Head, M. J. (1998). Temperature and Surface-Ocean Water Balance of the Mid-Holocene Tropical Western Pacific. *Science*, 279(5353), 1014-1018. <https://doi.org/doi:10.1126/science.279.5353.1014>
- Gallup, C. D., Edwards, R. L., & Johnson, R. G. (1994). The timing of high sea levels over the past 200,000 years. *Science*, 263(5148), 796-800. <https://doi.org/10.1126/science.263.5148.796>
- 560 Gonzalez-De Zayas, R., Merino-Ibarra, M., Soto-Jimenez, M. F., & Castillo-Sandoval, F. S. (2013). Biogeochemical responses to nutrient inputs in a Cuban coastal lagoon: runoff, anthropogenic, and groundwater sources. *Environ Monit Assess*, 185(12), 10101-10114. <https://doi.org/10.1007/s10661-013-3316-y>
- Greve, S., Frank, N., Montagna, P., Winter, A., Rico-Esenaro, S. D., Carricart-Ganivet, J. P., & Hetzinger, S. (in prep.). Precision measurement of $\delta^{234}\text{U}$ in annually banded tropical corals. *Geochronology*.
- 565 Grzymko, T. J., Marcantonio, F., McKee, B. A., & Mike Stewart, C. (2007). Temporal variability of uranium concentrations and $^{234}\text{U}/^{238}\text{U}$ activity ratios in the Mississippi river and its tributaries. *Chemical Geology*, 243(3-4), 344-356. <https://doi.org/10.1016/j.chemgeo.2007.05.024>
- Haase-Schramm, A., Böhm, F., Eisenhauer, A., Dullo, W.-C., Joachimski, M. M., Hansen, B., & Reitner, J. (2003). Sr/Ca ratios and oxygen isotopes from sclerosponges: Temperature history of the Caribbean mixed layer and thermocline during the Little Ice Age. *Paleoceanography*, 18(3). <https://doi.org/https://doi.org/10.1029/2002PA000830>
- 570 Harbott, M., Wu, H. C., Kuhnert, H., Jimenez, C., González-Díaz, P., & Rixen, T. (2023). A Warming Southern Gulf of Mexico: Reconstruction of Anthropogenic Environmental Changes From a *Siderastrea siderea* Coral on the Northern Coast of Cuba. *Paleoceanography and Paleoclimatology*, 38(12), e2023PA004717. <https://doi.org/https://doi.org/10.1029/2023PA004717>
- 575 Hathorne, E. C., Felis, T., James, R. H., & Thomas, A. (2011). Laser ablation ICP-MS screening of corals for diagenetically affected areas applied to Tahiti corals from the last deglaciation. *Geochimica et Cosmochimica Acta*, 75(6), 1490-1506. <https://doi.org/https://doi.org/10.1016/j.gca.2010.12.011>
- Haug, H. G., Konrad, A. H., Daniel, M. S., Larry, C. P., & Ursula, R. (2001). Southward Migration of the Intertropical Convergence Zone Through the Holocene. *Science*, 293(5533), 1304-1308. <https://doi.org/10.1126/science.1059725>
- 580 Henderson, G. M. (2002). Seawater ($^{234}\text{U}/^{238}\text{U}$) during the last 800 thousand years. *Earth and Planetary Science Letters*, 199(1), 97-110. [https://doi.org/https://doi.org/10.1016/S0012-821X\(02\)00556-3](https://doi.org/https://doi.org/10.1016/S0012-821X(02)00556-3)
- Henderson, G. M., Cohen, A. S., & O'Nions, R. K. (1993). $^{234}\text{U}/^{238}\text{U}$ ratios and ^{230}Th ages for Hateruma Atoll corals: implications for coral diagenesis and seawater $^{234}\text{U}/^{238}\text{U}$ ratios. *Earth and Planetary Science Letters*, 115(1), 65-73. [https://doi.org/https://doi.org/10.1016/0012-821X\(93\)90213-S](https://doi.org/https://doi.org/10.1016/0012-821X(93)90213-S)
- 585 Henderson, G. M., & Slowey, N. C. (2000). Evidence from U-Th dating against Northern Hemisphere forcing of the penultimate deglaciation. *Nature*, 404(6773), 61-66. <https://doi.org/10.1038/35003541>
- Hitchcock, G. L., Wiseman, W. J., Boicourt, W. C., Mariano, A. J., Walker, N., Nelsen, T. A., & Ryan, E. (1997). Property fields in an effluent plume of the Mississippi river. *Journal of Marine Systems*, 12(1), 109-126. [https://doi.org/https://doi.org/10.1016/S0924-7963\(96\)00092-9](https://doi.org/https://doi.org/10.1016/S0924-7963(96)00092-9)
- 590 Hodell, D. A., Brenner, M., Curtis, J. H., Medina-González, R., Idefonso-Chan Can, E., Albornaz-Pat, A., & Guilderson, T. P. (2005). Climate change on the Yucatan Peninsula during the Little Ice Age. *Quaternary Research*, 63(2), 109-121. <https://doi.org/10.1016/j.yqres.2004.11.004>
- 595 Horwitz, E. P., Dietz, M. L., Chlantzla, R., & Diamond, H. (1992). Separation and preconcentration of uranium from acidic media by extraction chromatography. *Analytica Chimica Acta*, 226, 25-37.

- Hu, H.-M., Shen, C.-C., Cheng, H., Woodhead, J. D., Edwards, R. L., Zhao, J.-x., Huang, C.-Y., Lu, P.-Y., Chien, W.-Y., Wang, J., Jia, X., Yokoyama, Y., Cai, Y., & Zachariáš, J. (2025). Sub-epsilon natural $^{234}\text{U}/^{238}\text{U}$ measurements refine the ^{234}U half-life and U-Th geochronology. *Science Advances*, *11*(40), eadu8117. <https://doi.org/doi:10.1126/sciadv.adu8117>
- 600 Iturralde-Vinent, M. A., García-Casco, A., Rojas-Agramonte, Y., Proenza, J. A., Murphy, J. B., & Stern, R. J. (2016). The geology of Cuba: A brief overview and synthesis. *GSA Today*, 4-10. <https://doi.org/10.1130/gsatg296a.1>
- Ivanovich, M., & Harmon, R. S. (1992). *Uranium-series disequilibrium: applications to earth, marine, and environmental sciences*. 2. ed. Oxford (United Kingdom); Clarendon Press; <https://doi.org/https://doi.org/> Other: ISBN: 0 19 854278 X GBN
- 605 Jaffey, A. H., Flynn, K. F., Glendenin, L. E., Bentley, W. C., & Essling, A. M. (1971). Precision Measurement of Half-Lives and Specific Activities of ^{235}U and ^{238}U . *Physical Review C*, *4*(5), 1889-1906. <https://doi.org/10.1103/PhysRevC.4.1889>
- Johns, W. E., Townsend, T. L., Fratantoni, D. M., & Wilson, W. D. (2002). On the Atlantic inflow to the Caribbean Sea. *Deep Sea Research Part I: Oceanographic Research Papers*, *49*(2), 211-243. [https://doi.org/https://doi.org/10.1016/S0967-0637\(01\)00041-3](https://doi.org/https://doi.org/10.1016/S0967-0637(01)00041-3)
- 610 Johnson, S. (2011). *Climate and Catastrophe in Cuba and the Atlantic World in the Age of Revolution*. University of North Carolina Press. https://doi.org/10.5149/9780807869345_johnson
- Kennett, D. J., Breitenbach, S. F. M., Aquino, V. V., Asmerom, Y., Awe, J., Baldini, J. U. L., Bartlein, P., Culleton, B. J., Ebert, C., Jazwa, C., Macri, M. J., Marwan, N., Polyak, V., Prufer, K. M., Ridley, H. E., Sodemann, H., Winterhalder, B., & Haug, G. H. (2012). Development and Disintegration of Maya Political Systems in Response to Climate Change. *Science*, *338*(6108), 788-791. <https://doi.org/doi:10.1126/science.1226299>
- 615 Kerber, I. K., Arps, J., Eichstädter, R., Kontor, F., Dornick, C., Schröder-Ritzrau, A., Babu, A., Warken, S., & Frank, N. (2023). Simultaneous U and Th isotope measurements for U-series dating using MCICPMS. *Nuclear Instruments & Methods in Physics Research Section B-Beam Interactions with Materials and Atoms*, *539*, 169-178. <https://doi.org/10.1016/j.nimb.2023.04.003>
- 620 Kerber, I. K., Kontor, F., Mielke, A., Warken, S., & Frank, N. (2025). Technical note: „U-Th Analysis” – an open-source software dedicated to MCICPMS U-series-data treatment and evaluation. *Geochronology*, *7*, 1–13. <https://doi.org/https://doi.org/10.5194/gchron-7-1-2025>
- Kigoshi, K. (1971). Alpha-Recoil Thorium-234: Dissolution into Water and the Uranium-234/Uranium-238 Disequilibrium in Nature. *Science*, *173*, 47-48.
- 625 Kilbourne, K. H., Quinn, T. M., Webb, R., Guilderson, T., Nyberg, J., & Winter, A. (2008). Paleoclimate proxy perspective on Caribbean climate since the year 1751: Evidence of cooler temperatures and multidecadal variability. *Paleoceanography*, *23*(3). <https://doi.org/10.1029/2008pa001598>
- Kipp, M. A., Li, H., Ellwood, M. J., John, S. G., Middag, R., Adkins, J. F., & Tissot, F. L. H. (2022). ^{238}U , ^{235}U and ^{234}U in seawater and deep-sea corals: A high-precision reappraisal. *Geochimica et Cosmochimica Acta*, *336*, 231-248. <https://doi.org/10.1016/j.gca.2022.09.018>
- 630 Ku, T.-L., Knauss, K. G., & Mathieu, G. G. (1977). Uranium in open ocean: concentration and isotopic composition. *Deep-Sea Research*, *24*, 1005-1017.
- Ladd, M., Viau, A., Way, R., Gajewski, K., & Sawada, M. (2018). Variations in precipitation in North America during the past 2000 years. *The Holocene*, *28*(4), 667-675. <https://doi.org/10.1177/0959683617735583>
- 635 Leaman, K. D., Vertes, P. S., Atkinson, L. P., Lee, T. N., Hamilton, P., & Waddell, E. (1995). Transport, potential vorticity, and current/temperature structure across Northwest Providence and Santaren Channels and the Florida Current off Cay Sal Bank. *Journal of Geophysical Research: Oceans*, *100*(C5), 8561-8569. <https://doi.org/https://doi.org/10.1029/94JC01436>
- 640 Leder, J. J., Swart, P. K., Szmant, A. M., & Dodge, R. E. (1996). The origin of variations in the isotopic record of scleractinian corals: I. Oxygen. *Geochimica et Cosmochimica Acta*, *60*(15), 2857-2870. [https://doi.org/https://doi.org/10.1016/0016-7037\(96\)00118-4](https://doi.org/https://doi.org/10.1016/0016-7037(96)00118-4)
- Li, L., Chen, J., Chen, T., Chen, Y., Hedding, D. W., Li, G., Li, L., Li, T., Robinson, L. F., West, A. J., Wu, W., You, C.-F., Zhao, L., & Li, G. (2018). Weathering dynamics reflected by the response of riverine uranium isotope disequilibrium

- 645 to changes in denudation rate. *Earth and Planetary Science Letters*, 500, 136-144.
<https://doi.org/10.1016/j.epsl.2018.08.008>
- Li, T., Robinson, L. F., MacGilchrist, G. A., Chen, T., Stewart, J. A., Burke, A., Wang, M., Li, G., Chen, J., & Rae, J. W. B. (2023). Enhanced subglacial discharge from Antarctica during meltwater pulse 1A. *Nature Communications*, 14(1), 7327. <https://doi.org/10.1038/s41467-023-42974-0>
- 650 Limia, M., Vega, R., & Pérez, R. (2003). Climatología de los ciclones tropicales que han afectado a Cuba y sus provincias. Memorias del X Congreso Latinoamericano e Ibérico de Meteorología “La meteorología y el desarrollo sostenible”. La Habana, Cuba,
- Lund, D. C., & Curry, W. (2006). Florida Current surface temperature and salinity variability during the last millennium. *Paleoceanography*, 21(2). <https://doi.org/https://doi.org/10.1029/2005PA001218>
- 655 Lund, D. C., Lynch-Stieglitz, J., & Curry, W. B. (2006). Gulf Stream density structure and transport during the past millennium. *Nature*, 444(7119), 601-604. <https://doi.org/10.1038/nature05277>
- Martinez, C., Goddard, L., Kushnir, Y., & Ting, M. (2019). Seasonal climatology and dynamical mechanisms of rainfall in the Caribbean. *Climate Dynamics*, 53(1), 825-846. <https://doi.org/10.1007/s00382-019-04616-4>
- Monzote, R. F. (2008). *From rainforest to cane field in Cuba: an environmental history since 1492*. Univ of North Carolina Press.
- 660 Monzote, R. F. (2024). Land Use in the Caribbean from the Mid-Nineteenth Century to 1950. *The Anthropocene as Multiple Crisis: Perspectives from Latin America*, 281.
- Morey, S. L., Martin, P. J., O'Brien, J. J., Wallcraft, A. A., & Zavala-Hidalgo, J. (2003). Export pathways for river discharged fresh water in the northern Gulf of Mexico. *Journal of Geophysical Research: Oceans*, 108(C10). <https://doi.org/https://doi.org/10.1029/2002JC001674>
- 665 Muller-Karger, F. E. (2000). The spring 1998 northeastern Gulf of Mexico (NEGOM) cold water event: Remote sensing evidence for upwelling and for eastward advection of Mississippi water (or: How an errant Loop Current anticyclone took the NEGOM for a spin). *Gulf of Mexico Science*, 18(1), 6.
- Not, C., Brown, K., Ghaleb, B., & Hillaire-Marcel, C. (2012). Conservative behavior of uranium vs. salinity in Arctic sea ice and brine. *Marine Chemistry*, 130-131, 33-39. <https://doi.org/https://doi.org/10.1016/j.marchem.2011.12.005>
- 670 Oey, L.-Y., Lee, H.-C., & Schmitz Jr., W. J. (2003). Effects of winds and Caribbean eddies on the frequency of Loop Current eddy shedding: A numerical model study. *Journal of Geophysical Research: Oceans*, 108(C10). <https://doi.org/https://doi.org/10.1029/2002JC001698>
- Osmond, J., & Cowart, J. (1976). The theory and uses of natural uranium isotopic variations in hydrology. *Atomic Energy Review*, 14(4), 621-679.
- 675 Osmond, J. K., & Cowart, J. B. (2000). U-Series Nuclides as Tracers in Groundwater Hydrology. In P. G. Cook & A. L. Herczeg (Eds.), *Environmental Tracers in Subsurface Hydrology* (pp. 145-173). Springer US. https://doi.org/10.1007/978-1-4615-4557-6_5
- Paces, J. B., Ludwig, K. R., Peterman, Z. E., & Neymark, L. A. (2002). 234U/238U evidence for local recharge and patterns of ground-water flow in the vicinity of Yucca Mountain, Nevada, USA. *Applied Geochemistry*, 17(6), 751-779. [https://doi.org/https://doi.org/10.1016/S0883-2927\(02\)00037-9](https://doi.org/https://doi.org/10.1016/S0883-2927(02)00037-9)
- 680 Palmer, M. R., & Edmond, J. M. (1993). Uranium in river water. *Geochimica et Cosmochimica Acta*, 57(20), 4947-4955. [https://doi.org/https://doi.org/10.1016/0016-7037\(93\)90131-F](https://doi.org/https://doi.org/10.1016/0016-7037(93)90131-F)
- Paterne, M., Druffel, E. R. M., Guilderson, T. P., Blamart, D., Moreau, C., Weil-Accardo, J., & Feuillet, N. (2023). Pulses of South Atlantic water into the tropical North Atlantic since 1825 from coral isotopes. *Science Advances*, 9(50), eadi1687. <https://doi.org/doi:10.1126/sciadv.adi1687>
- 685 Pourmand, A., Tissot, F. L. H., Arienzo, M., & Sharifi, A. (2014). Introducing a Comprehensive Data Reduction and Uncertainty Propagation Algorithm for U-Th Geochronometry with Extraction Chromatography and Isotope Dilution MC-ICP-MS. *Geostandards and Geoanalytical Research*, 38(2), 129-148. <https://doi.org/https://doi.org/10.1111/j.1751-908X.2013.00266.x>
- 690 Ren, L., Braddock, K. L., Gerard, M. W., Daniel, P. S., & Ove, H.-g. (2003). Deconvolving the $\delta^{18}\text{O}$ seawater component from subseasonal coral $\delta^{18}\text{O}$ and Sr/Ca at Rarotonga in the southwestern subtropical Pacific for the period 1726 to 1997. *Geochimica et Cosmochimica Acta*, 67(9), 1609-1621. [https://doi.org/https://doi.org/10.1016/S0016-7037\(02\)00917-1](https://doi.org/https://doi.org/10.1016/S0016-7037(02)00917-1)

- 695 Richey, J. N., Poore, R. Z., Flower, B. P., Quinn, T. M., & Hollander, D. J. (2009). Regionally coherent Little Ice Age cooling in the Atlantic Warm Pool. *Geophysical Research Letters*, 36(21). <https://doi.org/https://doi.org/10.1029/2009GL040445>
- Robinson, L. F., Belshaw, N. S., & Henderson, G. M. (2004b). U and Th concentrations and isotope ratios in modern carbonates and waters from the Bahamas. *Geochimica et Cosmochimica Acta*, 68(8), 1777-1789. <https://doi.org/10.1016/j.gca.2003.10.005>
- 700 Robinson, L. F., Henderson, G. M., Hall, L., & Matthews, I. (2004a). Climatic Control of Riverine and Seawater Uranium-Isotope Ratios. *Science*, 305, 851-854.
- Robinson, L. F., Henderson, G. M., & Slowey, N. C. (2002). U-Th dating of marine isotope stage 7 in Bahamas slope sediments. *Earth and Planetary Science Letters*, 196, 175-187.
- 705 Scholz, D., Mangini, A., & Felis, T. (2004). U-series dating of diagenetically altered fossil reef corals. *Earth and Planetary Science Letters*, 218(1), 163-178. [https://doi.org/https://doi.org/10.1016/S0012-821X\(03\)00647-2](https://doi.org/https://doi.org/10.1016/S0012-821X(03)00647-2)
- Schorndorf, N., Frank, N., Ritter, S. M., Warken, S. F., Scholz, C., Keppler, F., Scholz, D., Weber, M., Aviles Olguin, J., & Stinnesbeck, W. (2023). Mid- to late Holocene sea-level rise recorded in Hells Bells (234)U/(238)U ratio and geochemical composition. *Sci Rep*, 13(1), 10011. <https://doi.org/10.1038/s41598-023-36777-y>
- 710 Shen, C.-C., Lawrence Edwards, R., Cheng, H., Dorale, J. A., Thomas, R. B., Bradley Moran, S., Weinstein, S. E., & Edmonds, H. N. (2002). Uranium and thorium isotopic and concentration measurements by magnetic sector inductively coupled plasma mass spectrometry. *Chemical Geology*, 185, 165-178.
- Smith, J. M., Quinn, T. M., Helmle, K. P., & Halley, R. B. (2006). Reproducibility of geochemical and climatic signals in the Atlantic coral *Montastraea faveolata*. *Paleoceanography*, 21(1). <https://doi.org/https://doi.org/10.1029/2005PA001187>
- 715 Swarzenski, P., Campbell, P., Porcelli, D., & McKee, B. (2004). The estuarine chemistry and isotope systematics of 234,238U in the Amazon and Fly Rivers. *Continental Shelf Research*, 24(19), 2357-2372. <https://doi.org/https://doi.org/10.1016/j.csr.2004.07.025>
- Swarzenski, P. W., & Baskaran, M. (2007). Uranium distribution in the coastal waters and pore waters of Tampa Bay, Florida. *Marine Chemistry*, 104(1), 43-57. <https://doi.org/https://doi.org/10.1016/j.marchem.2006.05.002>
- 720 Terry, J. P., & Kim, I.-H. (2015). Morphometric analysis of tropical storm and hurricane tracks in the North Atlantic basin using a sinuosity-based approach. *International Journal of Climatology*, 35(6), 923-934. <https://doi.org/https://doi.org/10.1002/joc.4027>
- Thompson, W. G., Spiegelman, M. W., Goldstein, S. L., & Speed, R. C. (2003). An open-system model for U-series age determinations of fossil corals. *Earth and Planetary Science Letters*, 210(1), 365-381. [https://doi.org/https://doi.org/10.1016/S0012-821X\(03\)00121-3](https://doi.org/https://doi.org/10.1016/S0012-821X(03)00121-3)
- 725 Viau, A. E., Gajewski, K., Sawada, M. C., & Fines, P. (2006). Millennial-scale temperature variations in North America during the Holocene. *Journal of Geophysical Research: Atmospheres*, 111(D9). <https://doi.org/https://doi.org/10.1029/2005JD006031>
- 730 Villemant, B., & Feuillet, N. (2003). Dating open systems by the 238U-234U-230Th method: application to Quaternary reef terraces. *Earth and Planetary Science Letters*, 210(1), 105-118. [https://doi.org/https://doi.org/10.1016/S0012-821X\(03\)00100-6](https://doi.org/https://doi.org/10.1016/S0012-821X(03)00100-6)
- Vorosmarty, C. J., Fekete, B. M., & Tucker, B. A. (1998). Global River Discharge, 1807-1991, V[ersion]. 1.1 (RivDIS). In: ORNL Distributed Active Archive Center.
- 735 Vose, R. S., Schmoyer, R. L., Steurer, P., Peterson, T. C., Heim, R., Karl, T. R., & Eischeid, J. K. (1992). The Global Historical Climatology Network: Long-term monthly temperature, precipitation, sea level pressure, and station pressure data.
- Wang, C., & Enfield, D. B. (2001). The Tropical Western Hemisphere Warm Pool. *Geophysical Research Letters*, 28(8), 1635-1638. <https://doi.org/https://doi.org/10.1029/2000GL011763>
- Wang, C., Lee, S.-K., & Enfield, D. B. (2008). Climate Response to Anomalously Large and Small Atlantic Warm Pools during the Summer. *Journal of Climate*, 21(11), 2437-2450. <https://doi.org/https://doi.org/10.1175/2007JCLI2029.1>
- 740 Wang, L., Ma, Z., Sun, Z., Wang, Y., Wang, X., Cheng, H., & Xiao, J. (2017). U concentration and 234 U/ 238 U of seawater from the Okinawa Trough and Indian Ocean using MC-ICPMS with SEM protocols. *Marine Chemistry*, 196, 71-80. <https://doi.org/10.1016/j.marchem.2017.08.001>

- 745 Wefing, A.-M., Arps, J., Blaser, P., Wienberg, C., Hebbeln, D., & Frank, N. (2017). High precision U-series dating of scleractinian cold-water corals using an automated chromatographic U and Th extraction. *Chemical Geology*, 475, 140-148. <https://doi.org/10.1016/j.chemgeo.2017.10.036>
- Winter, A., Ishioroshi, H., Watanabe, T., Oba, T., & Christy, J. (2000). Caribbean sea surface temperatures: Two-to-three degrees cooler than present during the Little Ice Age. *Geophysical Research Letters*, 27(20), 3365-3368. <https://doi.org/https://doi.org/10.1029/2000GL011426>
- 750 Zhang, T., Jiang, X., Liu, Q., Shang, T., Zhong, X., & Meng, C. (2023). Changes of active particulate uranium under the Water-Sediment Regulation Scheme in the lower Yellow River: Potential impact to the uranium flux into the global ocean. *Mar Pollut Bull*, 192, 115014. <https://doi.org/10.1016/j.marpolbul.2023.115014>
- 755 Zhou, J., Du, J., Moore, W. S., Qu, J., & Zhang, G. (2015). Concentrations and fluxes of uranium in two major Chinese rivers: The Changjiang River and the Huanghe River. *Estuarine, Coastal and Shelf Science*, 152, 56-64. <https://doi.org/10.1016/j.ecss.2014.11.004>